Micro-contact spectroscopy features of quasi-one-dimensional materials with a charge-density wave

2003 J. Phys. A: Math. Gen. 36 9311

(http://iopscience.iop.org/0305-4470/36/35/316)

INSTITUTE OF PHYSICS PUBLISHING JOURNAL OF PHYSICS A: MATHEMATICAL AND GENERAL

J. Phys. A: Math. Gen. **36** (2003) 9311–9322 PII: S0305-4470(03)58990-9

Micro-contact spectroscopy features of quasi-one-dimensional materials with a charge-density wave

A A Sinchenko[1], Yu I Latyshev[2], V Ya Pokrovskii[2], S G Zybtsev[2] and P Monceau[3]

[1] Moscow Engineering-Physics Institute, 115409 Moscow, Russia
[2] Institute of Radioengineering and Electronics, Russian Academy of Sciences, 103907 Moscow, Russia
[3] Centre de Recherches sur les très Basses Temperatures, BP 166, 38042 Grenoble, France

Received 30 January 2003, in final form 7 April 2003
Published 20 August 2003
Online at stacks.iop.org/JPhysA/36/9311

Abstract

We have applied the method of point-contact (PC) spectroscopy to conductors with a charge-density-wave (CDW) ground state. Recent experimental results of the investigation of characteristics of PC formed between a normal metal (N) and different CDW conductors are reported. For a uniform N–CDW boundary, we show that the interaction of carriers injected from the normal metal with the CDW results in their reflection without changes in the sign of the charge but with a momentum transfer $2p_F$ to the condensate of electron–hole pairs carried away from the N–CDW interface. In the case of a non-uniform N–CDW boundary (direct point contact), a strong local CDW deformation, due to a band bending effect, was observed in materials with a semiconducting ground state. The chemical potential can be strongly modified, changing the conductivity type in the vicinity of the PC. It was shown that, in the case of a CDW conductor with a metal or semimetal ground state, the band bending effect is negligible (because of the screening of the electric field by remaining normal carriers) and the spectroscopy of the Peierls energy gap is possible.

PACS numbers: 71.45.Lr, 73.40.Ns, 74.80.Fp

1. Introduction

It is well known that, as the temperature is reduced, a Peierls transition takes place in quasi-one-dimensional conductors, leading to the appearance of a superlattice—a charge- or spin-density wave—with a period equal to twice the electron Fermi wavelength of the original metal, $2p_F$. This transition yields a complete or partial dielectrilization of the electronic spectrum, in the vicinity of parts of the Fermi surface that are combined by the wave vector of the charge- or spin-density wave. Many properties of materials with a CDW, especially the collective

conduction mechanism which is associated with the motion of a charge (spin)-density wave under the influence of an electric field, have been comprehensively studied (for a review see [1]). However, a number of problems have not been studied in detail. One of them is the problem of contact phenomena in this type of material. Most CDW materials have a semiconducting ground state. So, in normal metal (N)–CDW contacts, one can expect similar effects as in semiconductors. On the other hand, the collective electronic state in CDW systems is in many aspects similar to that in superconductors, leading possibly to a similar effect as Andreev reflection. It seems very interesting to apply the method of point-contact (PC) spectroscopy to CDW systems, which is the direct method for investigating contact phenomena, as well as the peculiarities of the electronic spectrum [2].

In the present work, we describe some recent experimental results of effects taking place at an N–CDW boundary. In section 2, the physical mechanism for conversion of a normal carrier current into a CDW current at the uniform N–CDW interface is considered. In sections 3 and 4, we discuss the experimental results of direct PC investigations between a normal metal and a CDW with a semiconducting and a semimetal ground state, in the case of a non-uniform N–CDW boundary. The main conclusions are given in section 5.

2. Uniform N–CDW boundary

It is well known that at the metal (N)–superconductor (S) interface, Andreev reflection can occur, in which a particle incident from the normal metal changes its charge and all the momentum components upon reflection [3]. On the other hand, there is a formal analogy between CDW conductors and superconductors, since the condensed state in both is described by an order parameter $\Delta = |\Delta| \exp(\mathrm{i}\varphi)$ whose amplitude determines the energy gap in the spectrum of single-particle excitations, while the derivative of the phase (with respect to time in CDW conductors and with respect to position in superconductors) is proportional to the contribution of the condensed electrons to the electric current density. By analogy with superconductors, one can visualize a CDW as a condensate of bound pairs of electrons and holes whose momenta differ by the wave vector of the charge-density wave. This similarity leads one to expect an effect at an N–CDW interface analogous to the Andreev reflection in superconductors, i.e., the quantum transformation of the normal current to the CDW current when the energy of the particle incident from the normal metal is lower than the Peierls energy gap, and when there are no permitted quasi-particle states in the CDW.

The possibility of observing the sub-gap carrier reflection at an N–CDW interface was raised first by Kasatkin and Pashitzkii [4]; it was stated that the reflected particle must not change the sign of its charge but must, as in the case of a superconductor, reverse all its velocity components. Rejaei and Bauer examined the transport properties of N–CDW–N heterostructures [5, 6] and took into account the movement of the CDW condensate from the boundary when the incident electron is reflected. They also found that the reflection of a carrier from an N–CDW interface is not accompanied by a change of the sign of the charge of the reflected particle. However, it was shown that the electron–hole pairs moving from the interface carry away twice the momentum of the electron incident normal to the interface. This reflection mechanism can manifest itself only when the incident electron moves along the chain direction.

Another mechanism for the carrier reflection was proposed by Artemenko and Remizov [7] where they included the possibility of a mirror reflection of carriers incident on the N–CDW interface as well as a reflection at some angle determined by the projection of the CDW wave vector onto a plane perpendicular to the chain direction. The latter mechanism was referred to as a Bragg reflection from the electronic CDW crystal.

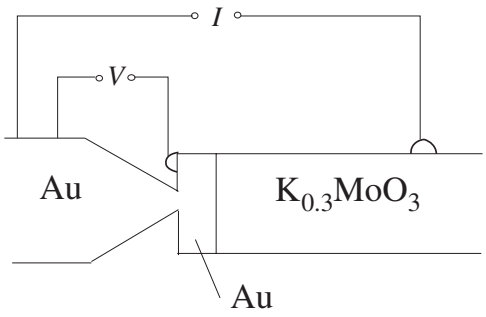

Figure 1. The experimental geometry for measuring carrier reflection at an N–CDW interface.

The direct method for the experimental observation of Andreev reflection is the van Kempen method proposed in [8]. In this method, a thin normal metal film with a thickness smaller than the electron mean free path is deposited over the interface of the investigated superconductor. Then, electrons injected into the normal film from a PC with a diameter d smaller than the N-layer thickness h reach the N–S interface ballistically. In the presence of Andreev reflection, most of them return as holes along the incident trajectories to the point contact, reducing the contact resistance by a factor of two in the ideal case. We have used this method in our works [9, 10] for searching for sub-gap reflection at an N–CDW interface. We measured single crystals $K_{0.3}MoO_3$ with the Peierls transition temperature $T_P = 183$ K. Point contacts were formed directly at low temperature ($T = 77$ K) between an Au tip and a thin gold layer, with a thickness $h = 50$ nm, evaporated on the crystal plane nearly perpendicular to the chain direction. The experiments were performed at $T = 77$ K which is well below the Peierls transition temperature for $K_{0.3}MoO_3$. The geometry of the experiment is shown in figure 1.

Figure 2 shows typical plots of the differential resistance $R_d = dV/dI$ as a function of the voltage V across several different PCs. For all contacts, the curve $R_d(V)$ emerges at high bias voltages V into a square-law dependence; the increment in resistance corresponds to a small Joule heating of the contact, and is determined by the resistance of the metal–metal contact $R_{dN}(V)$, as shown by the dashed curve in figure 2. Another type of nonlinearity is observed at low voltages. The $R_d(V)$ curves in this region have a minimum at $V = 0$ and maxima at $eV_0 = \pm\Delta_P$. To extract this nonlinearity, one needs to subtract the background dependence caused by Joule heating. Figure 3 shows the normalized dependence $R_d(V)/R_{dN}(V)$ for one of these contacts. It can be seen that the resulting curve is quite similar to the Andreev reflection spectrum for a superconductor [11], but it is symmetric relative to line $R_d(V)/R_{dN}(V) \equiv 1$. It can only happen in one case, when particles injected from the normal metal do not change the sign of their charge after reflection on the N–CDW interface. Another difference is that, in the case of a CDW, the amplitude of the effect is one order of magnitude smaller than in superconductors. It may be concluded that, in contrast to superconductors, the contribution to the PC resistance, because of the reflection at the N–CDW interface, does not come from all directions of injection, but only from a few. This result is in contradiction with the model [4] which predicted the reversibility of all velocity components of injected particles for any direction of injection.

Let us show now that the effect observed cannot be explained by the usual mirror reflection. Figure 4(a) illustrates schematically the processes which take place at the N–CDW interface. If the observed effect is only attributed to the mirror reflection (it may be the mirror reflection

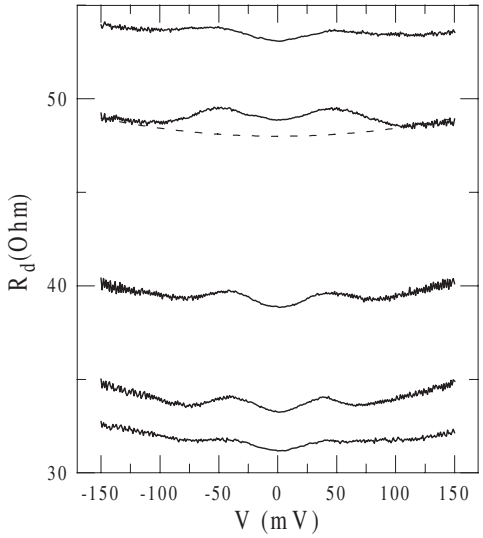

Figure 2. Differential resistance $R_d = dV/dI$ as a function of voltage V for Au–Au–$K_{0.3}MoO_3$ point contacts at $T = 77$ K.

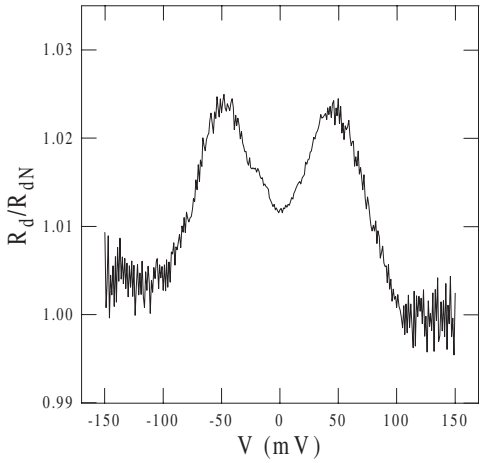

Figure 3. Normalized differential resistance R_d/R_{dN} as a function of voltage V for a given Au–Au–$K_{0.3}MoO_3$ point contact at $T = 77$ K.

on the Peierls energy gap barrier and on the barrier associated with the non-ideal interface), the excess resistance should have a step-like shape (figure 4(*b*)) with an amplitude determined by the relative number of reflected carriers going back after reflection through the PC. These particles are injected perpendicularly to the N–CDW interface, and their relative number is of the order of $(d/h)^2$, that explains the very small amplitude of the effect. However, in this case, there is no possibility of explaining the double-peak structure observed in our experiment because the reflections on the energy gap barrier and on the non-ideal interface are mixed up.

The observed shape of reflection spectra can be explained in the frame of the model described in [5, 6]. Indeed, it can be seen from figure 4(*a*) that if the chain direction is not

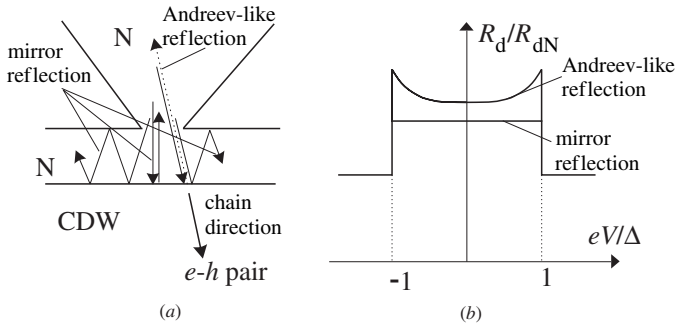

Figure 4. Diagram of the possible reflection processes on an N–CDW boundary (*a*); and qualitative point-contact spectra for mirror and Andreev-like reflections (*b*).

exactly perpendicular to the N–CDW interface (as it is in the real experimental situation), for the injection direction coincident with the chain direction, the reflections on the energy gap barrier and on the non-ideal interface are distinct. In this case, the mirror-reflected particles do not give any contribution to the PC resistance. On the other hand, the probability of the mirror reflection decreases with the increase of energy, while the probability of reflection due to the energy gap barrier (Andreev-like reflection) increases [12]. So, one has an additional contribution to the PC resistance which has maxima at $V = \pm\Delta_P/e$ (figure 4(*b*)).

In principle, the model in [7] gives the same result. Following this model, the additional contribution to the PC resistance comes from the trajectory corresponding to the Bragg reflection. However, using the known lattice parameters and the CDW wave vector in $K_{0.3}MoO_3$ [13], we estimate the angle corresponding to this trajectory to be $\alpha \approx 40$–50°. In this case, the path length from the PC to the N–CDW interface is larger than the mean free path and, because of scattering, the contribution to the PC resistance is negligibly small.

Thus, the observed experimental results indicate a non-trivial character of the interaction of normal carriers with a CDW condensate at the N–CDW boundary.

3. Direct N–CDW point contacts. Materials with a semiconducting ground state

We have considered above the situation of a uniform N–CDW boundary. It was shown in [14] that, in this case, the screening of the electric field takes place over a small length which is of the order of the Thomas–Fermi length. Another situation occurs in the case of a direct N–CDW point contact, which can be considered as a non-uniform perturbation. As was shown in [15, 16], the defects of such type can produce a strong bending of the energy bands for CDW materials with a semiconducting ground state. When the CDW is at rest, the transport properties are determined by the electron and the hole excitations through the Peierls energy gap. The charge of quasi-particles $e(p - n)$ changes if the CDW wave vector q changes: $q - q(T = 0) = \frac{1}{\pi}(p - n)$ [17]. When an electric field less than the threshold electric field E_T for depinning the CDW is applied to a Peierls semiconductor, a distortion of the CDW occurs in the vicinity of the contacts. This CDW deformation changes the electron and hole densities. It means that the CDW with a semiconducting ground state can be viewed as a conventional semiconductor but with a variable degree of doping depending on external perturbations. As the electric field increases further, the deformation of the CDW achieves a critical value, phase slip (PS) centres form in the vicinity of contact, and the CDW motion starts. If the contact area is large, the shift of the chemical potential ζ in the vicinity of contacts

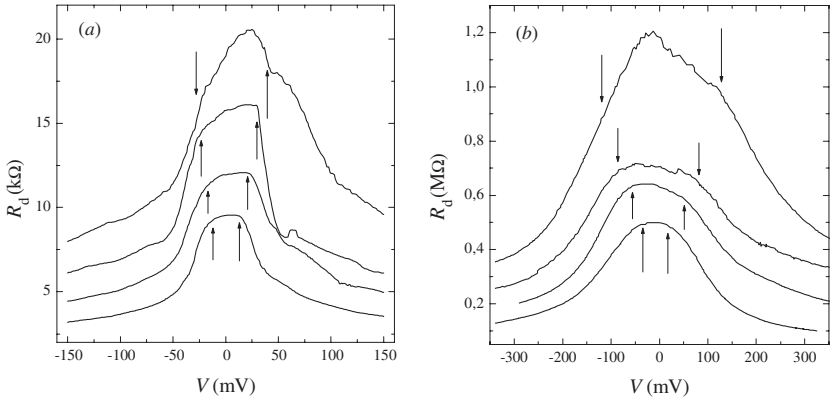

Figure 5. $R_d(V)$ dependences for relatively low-resistance point contacts Cu–$K_{0.3}MoO_3$ (*a*); and Cu–TaS_3 (*b*) at $T = 77$ K. Arrows indicate the voltages corresponding to the critical deformation of the CDW.

is insignificant ($<kT$). A different situation may occur in the vicinity of a micro-contact with a size $a < 100$ Å. The length of the CDW distortion is of the same order of magnitude, because the electric field is localized near the point contact in a region with a characteristic size $\sim a$ [18]. In this case, when a PS occurs, the change in q can be estimated as $\delta q = 2\pi/a$, and the corresponding $\delta\zeta_{2\pi} \approx \delta q(\delta\zeta/\mathrm{d}q) \approx kT(\delta q/q)(R(T)/R(300\ \mathrm{K}))$ [19]. This value for typical Peierls conductors, for example, for $K_{0.3}MoO_3$ or TaS_3, is many times higher than kT practically at all temperatures. Thus, even a single PS event shifts the chemical potential by a large value. So, it may be considered that a very large CDW distortion and a shift of the chemical potential can occur in the vicinity of an N–CDW point contact of sufficiently small area.

For the experimental investigation of processes which take place in an N–CDW micro-contact, we have measured the differential current–voltage (IV) characteristics of point contacts between a normal metal (Au, Cu) and $K_{0.3}MoO_3$ and TaS_3 single crystals. All contacts were oriented along the chain direction. The experiments were performed at $T = 77$ K, which is well below the Peierls transition temperatures of both materials (183 K for $K_{0.3}MoO_3$ and 220 K for TaS_3).

Figure 5 shows $R_d(V)$ curves for Cu–$K_{0.3}MoO_3$ (*a*) and Cu–TaS_3 (*b*) contacts with relatively low resistances (large point-contact diameter). At a certain voltage, a sharp decrease of the differential resistance (indicated by arrows) is observed for all shown curves. We associate this singularity with the critical deformation of the CDW, that is the onset of PS. It can be seen that the voltage corresponding to this process increases rapidly with the growth of point-contact resistance. So, we can hope that for high-resistance contacts it could be possible to observe elastic deformations of the CDW (without PS) in a wide range of bias voltages. In this case, we could comprehensively study the local CDW distortions and experimentally verify the applicability of the model [17].

Several typical dependences $R_d(V)$ of various high-resistance point contacts at $T = 77$ K are displayed in figure 6 for $K_{0.3}MoO_3$ (*a*) and TaS_3 (*b*). In contrast with the contact characteristics shown in figure 5, $R_d(V)$ varies smoothly; that is, the CDW remains static in the entire range of applied voltages. A maximum of the resistance is observed in all curves at $V = V_0 > 0$ for $K_{0.3}MoO_3$, and $V_0 < 0$ for TaS_3. By changing the contact diameter and temperature, V_0 varied non-systematically within a small range of voltages.

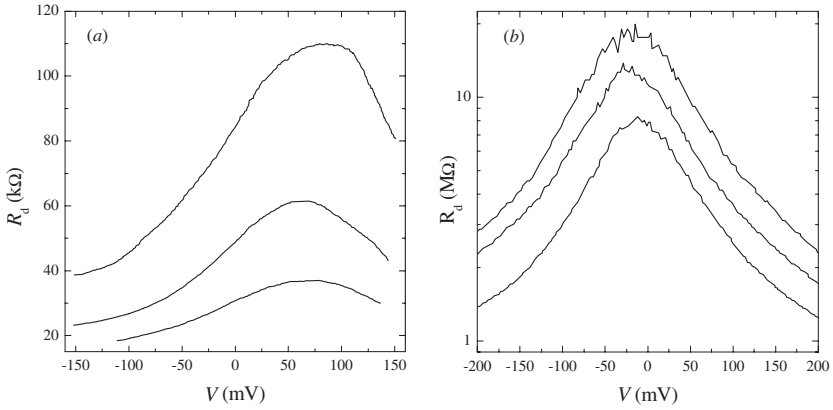

Figure 6. $R_d(V)$ dependences for high-resistance point contacts Cu–$K_{0.3}MoO_3$ (*a*); and Cu–TaS_3 (*b*) at $T = 77$ K.

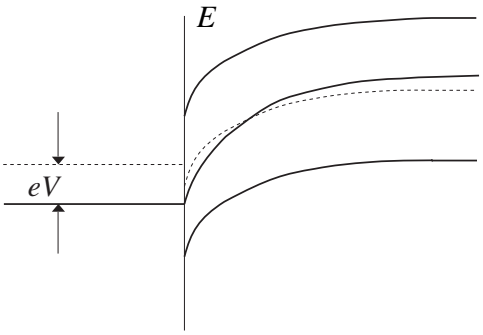

Figure 7. Schematic diagram of energy bands in the vicinity of an N–CDW point contact for an n-type Peierls conductor at $V > V_0$. The dashed line designates the effective middle of the Peierls energy gap.

Let us show now that the change in the point-contact resistance can be well described within the framework of the semiconducting model of the CDW [17]. The following qualitative picture stems from these results: a CDW distortion δq leads to the partial screening of the electric field in the vicinity of the contact. This yields a shift of the chemical potential $\delta\zeta \approx \delta q(\delta\zeta/\mathrm{d}q)$ and a change in resistance. A maximum of the resistance corresponds to the position of the chemical potential in the effective midgap ($\mu_n n = \mu_p p$, where μ_n and μ_p are the mobilities of electrons and holes, respectively). It is known from thermopower and Hall-effect measurements that $K_{0.3}MoO_3$ has a n-type conductivity [20], while TaS_3 is p-type [21, 22]. Indeed, as can be seen from figure 6, the maximum of $R_d(V)$ is observed at a positive voltage for $K_{0.3}MoO_3$ and at a negative voltage for TaS_3. The schematic diagram of energy bands in the vicinity of a point contact for a n-type CDW semiconductor is shown in figure 7. The positive sign of V_0 corresponds to a downwards shift of ζ (assuming that $\delta\zeta > 0$, which corresponds to a stretch of the CDW, $\delta q < 0$). It is evident from figure 7 that the CDW distortion tends to screen (decrease) the electric field determined by the gradient of the electrostatic potential (dashed curve in figure 7) near the contact. At $V > 0$, the chemical potential near the N–CDW interface drops and, in principle, can drop below the midgap in the

case of a sufficiently large CDW distortion. It is interesting to note that a variable p–n junction forms in a subsurface layer resulting from the contact of the CDW with a metal.

4. Direct N–CDW point contacts. Materials with a semi-metallic ground state

It was shown above, that for CDWs with a semiconducting ground state, the electric field in the vicinity of an N–CDW point contact penetrates into the CDW on a macroscopic length, leading to a strong band bending effect. The consequence of that is a significant non-symmetry of the IV curves of N–CDW point contacts. However, for CDW materials with a metal or semimetal ground state, the screening by the remaining normal carriers may be more effective. So, one can expect that the band bending effect will not be experimentally detectable in this case and, thus, the nonlinearity of IV curves of N–CDW point contacts will be determined by the interaction of carriers injected from the normal metal with the Peierls energy gap barrier, as in the case of a uniform N–CDW boundary.

We used $NbSe_3$ as a typical CDW conductor with a semimetal ground state. This compound is characterized by two Peierls transitions, which occur at $T_{P1} = 144$ K and $T_{P2} = 59$ K. In the low-temperature Peierls state, the Fermi surface retains some regions where the nesting conditions are not satisfied (the 'pockets') and, hence, providing the metallic conductivity [1]. The single crystals selected for experiments had sizes along the b-axis $L_b \approx$ 3–4 mm, along the c-axis $L_c \approx 10$–$50\ \mu$m and along the a^*-axis $L_a \approx 1\ \mu$m.

The specific form of $NbSe_3$ samples makes the formation of a point contact along the most interesting direction, that is the chain direction, practically impossible using the conventional metallic needle-type tip. But, according to [23], at low temperatures, the conductivity ratio $\sigma_b/\sigma_{a^*} \sim 10^4$. Therefore, for contacts oriented along the a^*-axis (the preparation of the contact is simple in this direction), the electric field distribution is strongly modified in the contact region in comparison with the isotropic case, and the preferable direction for the carrier injection is along the b-axis, which gives the possibility of interpreting the characteristics of N-$NbSe_3$ point contacts oriented along the a^*-axis as, in fact, being b-axis oriented contacts.

A typical example of IV-characteristics for point contacts oriented along a^* at $T = 3.6$ K is shown in figure 8. It may be seen that the increment of R_d at high voltages ($V > 100$ mV) is proportional to the square of the bias voltage, which is typical for Joule heating of a metal–metal contact (dotted line in figure 8). It is quite different from the tunnel-type IV curves for which the increment of resistance $\delta R_d(V) \sim 1/V^2$ [2]. This fact demonstrates, indeed, that these investigated contacts are of a direct type (without insulating barrier).

At $|V| < 100$ mV, the differential resistance grows in two steps, up to its maximum at $V = 0$. We associate these two-step maxima with the excess resistance arising from the reflection of the injected quasi-particles on the Peierls energy gap barriers. The first step in the excess resistance, corresponding to the carrier reflection on the first Peierls gap, Δ_{P1}, takes place for different contacts and samples at $|V_1| \approx 75$–85 mV. The second step is associated with the second Peierls gap, Δ_{P2}, and occurs at $|V_2| \approx 24$–30 mV. Indeed, the measured magnitudes of eV_1 and eV_2 corresponding to these singularities are in agreement with the values of the first and the second energy gaps of $NbSe_3$ determined earlier [25–28]. To make clearer the effect of carrier reflection on the energy gap barriers, we have normalized the $R_d(V)$ curve to the normal state background curve (shown as a dotted line in figure 8). The result of this procedure is shown in figure 9 (the solid line).

The temperature evolution of the normalized $R_d(V)$ dependence is shown in figure 10 for one of the a^*-axis contacts. It can be seen that, when the temperature is increased, the amplitude of the second step in the excess resistance decreases and its voltage position goes monotonically to zero; this step vanishes completely at $T = 59$ K, corresponding to the second

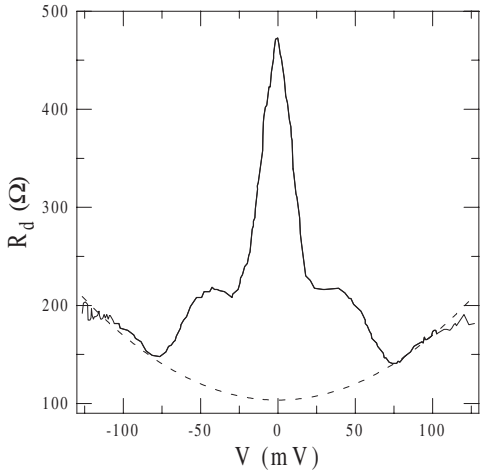

Figure 8. Typical variation of the differential resistance $R_{\rm d}(V)$ as a function of the applied voltage for a contact Au–$NbSe_3$ oriented along the a^*-axis direction measured at $T = 3.6$ K. The dotted line is the normal state background curve.

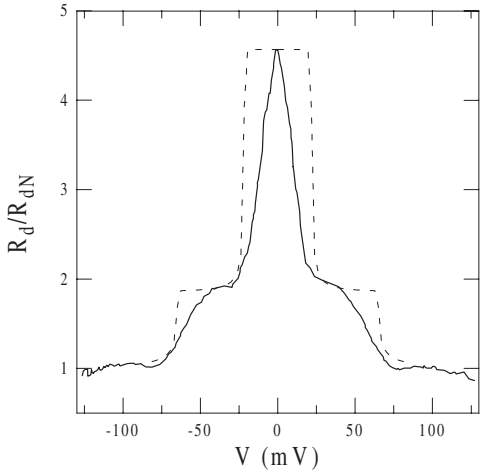

Figure 9. Normalized differential resistance $R_{\rm d}(V)/R_{\rm dN}(V)$ measured at $T = 3.6$ K for a contact Au–$NbSe_3$ oriented along the a^*-axis. The dotted line is the theoretical fit with $\Delta_{\rm P1} = 65.0$ mV and $\Delta_{\rm P2} = 24.0$ mV.

Peierls transition temperature. At the same time, the voltage position and the amplitude of the first step in the excess resistance remains practically unchanged in this temperature range (in accordance with the BSC-theory prediction). Indeed, according to this model, the first Peierls gap is practically independent of temperature in this temperature range.

Let us analyse the shape of the obtained point contact spectra. It can be seen from figure 9 that the result of the interaction of quasi-particles injected from the normal metal with the Peierls energy gaps reveals itself in the IV curves as an excess resistance at $|eV| < \Delta$. That is quite different from a tunnel-type junction where the energy gap singularity appears as a sharp minimum at $|eV| = \Delta$, demonstrating the features of the BCS-type tunnel density of states which diverges at $\pm\Delta$. The behaviour observed in our experiments is in qualitative

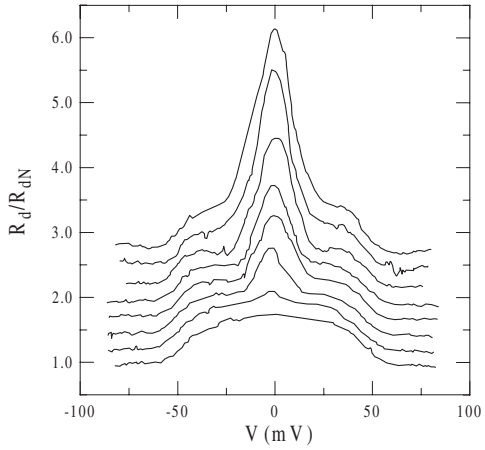

Figure 10. $R_{\rm d}/R_{\rm dN}(V)$ curves for a contact In–$NbSe_3$ oriented along the a^*-axis direction at $T =$ 4.2, 29.5, 48.2, 50.5, 52.6, 54.6, 58.3 and 60.4 K. The resistance scale corresponds to the curve at 60.4 K, the other curves are offset for clarity.

agreement with the models predicting the reflection of normal carriers from the energy gap barrier at the normal metal–CDW interface [5, 6].

For all the investigated contacts, we observe simultaneously the energy gap singularities corresponding to the low- and high-temperature CDW of $NbSe_3$. It is an indication that the first and the second Peierls transitions take place on different types of chains. Therefore, we can model our contact as two CDWs connected in parallel and a normal metal corresponding to the uncondensed remaining carriers. Then the total current through the contact, $I_{\rm t}$, is the sum of three currents:

$$I_{\rm t} = I_{\rm P1} + I_{\rm P2} + I_{\rm n} \tag{1}$$

where $I_{\rm P1}$, $I_{\rm P2}$ are the currents flowing through the parts of the contact including the first and the second CDW, and $I_{\rm n}$ is the current of the remaining normal carriers (not normal excitations of the CDWs). We assume that $I_{\rm n}(V)$ follows the Ohmic law and that the $I_{\rm P}(V)$ dependences may be calculated as

$$I_{\rm P}(V) = N(0)ev_{\rm F}A\int_{-\infty}^{\infty}[f_0(E-eV) - f_0(E)]D(E)\,{\rm d}E \tag{2}$$

where $f_0(E)$ is the electron distribution function, $N(0)$ is the density of states at the Fermi level, $v_{\rm F}$ is the Fermi velocity, A is the effective cross-section area corresponding to transport through the given CDW and $D(E)$ is the transmission coefficient, which depends on the corresponding CDW energy gap. The parameter A is proportional to the relative number of chains of a given type included in the contact. This parameter determines the relation between the amplitudes of the first and the second excess resistance maxima which are different for different point contacts.

Modelling the energy gap as a potential step with a height equal to $\Delta_{\rm P}$, we can consider our point contact as a quantum mechanical task about the scattering of a particle on such a type of barrier. The transmission coefficient obtained from the solution of the Schrödinger equation is

$$D(E) = \begin{cases} 0 & \text{for} \quad E \leqslant \Delta_{\rm P} \\ \frac{4\sqrt{E(E-\Delta_{\rm P})}}{(\sqrt{E}+\sqrt{E-\Delta_{\rm P}})^2} & \text{for} \quad E > \Delta_{\rm P}. \end{cases} \tag{3}$$

In this simple model, we do not consider the influence of a possible non-ideality of the N–CDW boundary. As a first approximation, we have also assumed that the normal state differential conductivity for all types of chains is the same and that dI_n/dV is energy independent. In this case, only A and Δ_P are free parameters. Following this model, the curve shown in figure 9 by a dotted line is obtained with $\Delta_{P1} = 65.0$ meV and $\Delta_{P2} = 24.0$ meV. It can be seen from the figure that the conductivity of the contacts starts to increase from very low voltages, even at very low temperatures. Such a result is in qualitative agreement with the Huang and Maki calculations [29] of the density of states in $NbSe_3$ assuming a two-dimensional electronic spectrum. The same conclusion about the two-dimensional character of the electron spectrum in $NbSe_3$ was made in [30].

5. Conclusions

The experimental results of our investigations of point-contact characteristics between a normal metal and different quasi-one-dimensional conductors with a charge-density-wave (CDW) ground state demonstrate that point-contact spectroscopy gives rich information about the physical properties of CDWs. We have shown that, for a uniform N–CDW boundary, the result of interaction of the carriers injected from the normal metal with a CDW is their reflection without change in the sign of their charge and with a momentum transfer $2p_F$ to the condensate of electron–hole pairs carried away from the N–CDW interface. We have also shown that for CDW materials with a semiconducting ground state a hysteresis-free CDW distortion is observed in the vicinity of the direct N–CDW point contact, leading to a change in conductivity. In this case, the chemical potential can be varied over a wide range by changing the conductivity from n-type to p-type. For contacts between a normal metal and a CDW material with a partially dielectrized electronic spectrum (semimetal ground state, as $NbSe_3$), we have clearly observed the reflection of carriers injected from the normal metal on the Peierls energy gap barriers (Andreev-like reflection), giving the possibility of direct energy gap spectroscopy. Our results show that the density of states in $NbSe_3$ corresponds to the two-dimensional character of the electronic spectrum in this material.

Acknowledgments

The authors thank S N Artemenko, L N Bulaevski, S V Zaitsev-Zotov and K Maki for helpful discussions of their experimental results. The work has been supported by Russian State Fund for Basic Research (grants no 01-02-16321, no 02-02-17263 and no 02-02-17301), INTAS (grant no 01-0474), the twinning programme no 19 between CRTBT-CNRS and RAS, and Russian Federal Program 'Integration' (Project B-0048).

References

[1] Grüner G 1994 *Density Waves in Solids* (Reading, MA: Addison-Wesley)
Gor'kov L and Grüner G 1989 *Charge Density Waves in Solids* (Amsterdam: Elsevier)
Gor'kov L and Grüner G 2002 *Electronic Crystals 02* ed S Brazovskii and P Monceau (*J. Physique France* **12**)
[2] Wolf E L 1985 *Principles of Electron Tunneling Specrtoscopy* (Oxford/New York: Oxford University Press/Clarendon)
[3] Andreev A F 1964 *Zh. Eksp. Teor. Fiz.* **46** 1823 (Engl. transl. 1964 *Sov. Phys.–JETP* **19** 1228)
[4] Kasatkin A L and Pashitzkii E A 1984 *Fiz. Nizk. Temp.* **10** 1222 (Engl. transl. *Sov. J. Low. Temp. Phys.* **10** 640)
[5] Visscher M I and Bauer G E W 1996 *Phys. Rev.* B **54** 2798
[6] Rejaei B and Bauer G E W 1996 *Phys. Rev.* B **54** 8487
[7] Artemenko S N and Remizov S V 1997 *Pis. Zh. Eksp. Teor. Fiz.* **65** 50 (Engl. transl. 1997 *JETP Lett.* **65** 53)

[8] van Son P C, van Kempen H and Wyder P 1987 *Phys. Rev. Lett.* **59** 2226
[9] Sinchenko A A, Latyshev Yu I, Zybtsev S G, Gorlova I G and Monceau P 1996 *Pis. Zh. Eksp. Teor. Fiz.* **64** 259 (Engl. transl. 1996 *JETP Lett.* **64** 285)
[10] Sinchenko A A, Latyshev Yu I, Zybtsev S G and Gorlova I G 1998 *Zh. Eksp. Teor. Fiz.* **113** 1830 (Engl. transl. 1998 *JETP* **86** 1001)
[11] Hoevers H F C, van der Grinten M G D, Jennen P L H, van Kempen H and van Son P C 1994 *J. Phys: Condens. Matter* **6** 65
[12] Blonder G E, Tinkham M and Klapwijk T M 1982 *Phys. Rev.* B **25** 4515
[13] Chedira M, Chenavas J, Marezio M and Marcus J 1985 *J. Solid State Chem.* **57** 300
[14] Artemenko S N and Volkov A F 1984 *Zh. Eksp. Teor. Fiz.* **87** 691 (Engl. transl. 1984 *Sov. Phys.–JETP* **60** 395)
[15] Artemenko S N and Gleisberg F 1995 *Phys. Rev. Lett.* **75** 497
[16] Artemenko S N 1997 *Zh. Eksp. Teor. Fiz.* **111** 1494 (Engl. transl. 1997 *JETP* **84** 823)
[17] Artemenko S N, Pokrovskii V Ya and Zaitsev-Zotov S V 1996 *Zh. Eksp. Teor. Fiz.* **64** 509 (Engl. transl. 1996 *JETP* **83** 590)
[18] Kulik I O, Omel'yanchuk A N and Shekhter R I 1977 *Fiz. Nizk. Temp.* **3** 1543 (Engl. transl. 1977 *Sov. J. Low. Temp. Phys.* **3** 740)
[19] Pokrovskii V Ya and Zaitsev-Zotov S V 1989 *Synth. Met.* **32** 321
[20] Schlenker C (ed) 1989 *Low-Dimensional Electronic Properties of Molybdenum Bronzes and Oxides* (Dordrecht: Kluwer)
[21] Higgs A W 1985 *Springer Lecture Notes in Physics* vol 217 ed G Hutirai and J Solyom (Berlin: Springer) p 422
[22] Latyshev Yu I, Savitskaya Ya S and Frolov V V 1983 *Pis. Zh. Eksp. Teor. Fiz.* **38** 446 (Engl. transl. 1983 *JETP Lett.* **38** 541)
[23] Latyshev Yu I, Monceau P, Laborde O, Pennetier B, Pavlenko V N and Yamashita T 1999 *J. Phys. IV France* **9** Pr-165
[24] Ekino T and Akimitsu J 1987 *J. Appl. Phys.* **26** 625
[25] Ekino T and Akimitsu J 1994 *Physica* B **194–6** 1221
[26] Dai Zhenxi, Slough C G and Coleman R V 1991 *Phys. Rev. Lett.* **66** 1318
[27] Fournel A, Sorbier J P, Konczykovski M and Monceau P 1986 *Phys. Rev. Lett.* **57** 2199
[28] Sinchenko A A, Latyshev Yu I, Zybtsev S G, Gorlova I G and Monceau P 1999 *Phys. Rev.* B **60** 4624
[29] Huang X Z and Maki K 1989 *Phys. Rev.* B **40** 2575
[30] Latyshev Yu I, Sinchenko A A, Bulaevski L N, Pavlenko V N and Monceau P 2002 *Pis. Zh. Eksp. Teor. Fiz.* **75** 93 (Engl. transl. *JETP Lett.* 2002 **75** 103)